Tight coupling between soil moisture and the surface radiation budget in semiarid environments: Implications for land-atmosphere interactions

Eric E. Small and Shirley A. Kurc

Department of Geological Sciences, University of Colorado, Boulder, Colorado, USA

Received 11 March 2002; revised 2 May 2003; accepted 20 June 2003; published 4 October 2003.

[1] Observations are used to examine how soil moisture influences the surface radiation budget, ground heat flux, and available energy in semiarid environments. Defining this relationship is critical to understand interactions between the land surface and the atmosphere, in particular assessing if a feedback exists between soil moisture and rainfall anomalies. We use two summers of data collected from semiarid grassland and shrubland ecosystems in central New Mexico. The response of surface radiation budget components and other variables to soil moisture variations are quantified via linear regression. Then, the variations are scaled over the observed range of soil moisture (15% volumetric water content). The soil temperature is lower by >10°C when the surface soil is wet, compared to when the soil is dry. This temperature decrease results in a measured decrease of 85–100 W m^{-2} in longwave radiation emitted at the surface. The increase in net longwave radiation is equal in magnitude because downward longwave radiation does not vary with soil moisture. The observed changes in net shortwave radiation are relatively minor (<10 W m^{-2}), as the surface albedo decreases by only 1.5% when soil is wet. Net radiation increases by an amount roughly equal to the decrease in emitted longwave radiation (~85–100 W m^{-2}). Changes in ground heat flux are not detectable, given the noise in the data. Therefore the available energy, Q_a, is higher by 80 W m^{-2} when the soil is wet. This change is 22% of average Q_a at the shrubland site and 19% at the grassland site. The observed soil moisture-induced Q_a variations are large compared to other sources of Q_a variability, so they should influence boundary layer moist static energy. However, the intervals during which soil moisture is high and therefore R_n and Q_a are enhanced are short, on the order of several days. Therefore feedbacks to rainfall may be limited. Compared to other environments, the influence of soil moisture on R_n and Q_a is likely greater in semiarid environments because soil moisture-induced fluctuations in evaporative fraction and surface temperature are relatively large. *INDEX TERMS:* 1818 Hydrology: Evapotranspiration; 1833 Hydrology: Hydroclimatology; 1866 Hydrology: Soil moisture; 3322 Meteorology and Atmospheric Dynamics: Land/atmosphere interactions; *KEYWORDS:* soil moisture, ground heat flux, soil temperature, net radiation, evapotranspiration, land-atmosphere interactions

Citation: Small, E. E., and S. A. Kurc, Tight coupling between soil moisture and the surface radiation budget in semiarid environments: Implications for land-atmosphere interactions, *Water Resour. Res.*, *39*(10), 1278, doi:10.1029/2002WR001297, 2003.

1. Introduction

[2] The state of the land surface affects the atmosphere above it via the surface-atmosphere fluxes of water, energy, and momentum [*Shukla and Mintz*, 1982; *Shuttleworth*, 1991; *Betts*, 2000]. Soil moisture strongly controls the nature of these fluxes, such as the partitioning of available energy between latent and sensible heating [*Entekhabi and Rodriquez-Iturbe*, 1994]. The soil moisture reservoir evolves on timescales as long as seasons, so soil moisture may act as a source of long-term "memory" of past precipitation events [*Entekhabi et al.*, 1992]. Because soil moisture both reflects past precipitation and influences the atmosphere, it has been hypothesized that a positive feedback may exist between soil moisture and rainfall: above (below) normal rainfall yields high (low) soil moisture, which in turn results in additional (limited) rainfall. If a positive soil moisture-rainfall feedback exists, then land surface memory due to soil moisture storage should amplify hydroclimatic variability, enhancing and prolonging both floods and droughts [*Entekhabi et al.*, 1992]. Modeling experiments [e.g., *Small*, 2001] and analysis of observations [e.g., *Findell and Eltahir*, 1997] are consistent with the presence of a positive soil moisture-rainfall feedback. However, the importance of these feedbacks in different environments and the processes that lead to them are difficult to constrain.

[3] One mechanism that could lead to a positive soil moisture-rainfall feedback is local precipitation recycling: high soil moisture enhances evapotranspiration (ET), which

0043-1397/03/2002WR001297$09.00

increases atmospheric water vapor, clouds and precipitation in that region [*Brubaker et al.*, 1993; *Eltahir and Bras*, 1996]. However, only a small fraction of the water evaporated from some area returns to the land surface as precipitation in that region [*Trenberth*, 1998]. In addition, the fraction of water that is locally recycled decreases as the spatial extent of the region examined decreases [*Eltahir and Bras*, 1996; *Trenberth*, 1998]. In contrast, soil moisture and surface flux anomalies should be most intense over relatively small areas. Therefore precipitation recycling is probably not a viable mechanism leading to feedbacks between soil moisture and rainfall.

[4] A more important pathway may result from the influence that soil moisture has on surface-atmosphere fluxes of water and energy and the state of the boundary layer (BL), and therefore the likelihood for convective precipitation [*Betts and Ball*, 1998; *Eltahir*, 1998; *Trenberth*, 1998]. The surface energy balance is summarized as

$$R_n - G = \lambda E + H = Q_a \tag{1}$$

where R_n is net radiation, G is ground heat flux, λE is latent heat flux, and H sensible heat flux (W m^{-2}). The available energy, Q_a, is the energy transferred from the land surface to the atmosphere via turbulent fluxes. It is equal to the net radiation absorbed by the surface minus the energy transferred into the ground. Evaporative fraction (EF) is the fraction of Q_a partitioned to latent heating (i.e., $\lambda E/Q_a$).

[5] *Betts and Ball* [1998] proposed a model explaining how soil moisture anomalies influence the BL and rainfall, based on data collected from the Konza Prairie during the First ISLSCP Field Experiment (FIFE) [*Sellers et al.*, 1992]. They proposed the following mechanism linking soil moisture and rainfall: (1) wet soil yields a high evaporative fraction (EF); (2) a high EF leads to a shallow BL; (3) the moist static energy (MSE) transferred from the surface to the atmosphere is concentrated in the BL because it is shallow and because entrainment of low MSE air from above the BL is limited; and (4) higher BL MSE increases the likelihood of convective precipitation [e.g., *Eltahir and Pal*, 1996]. This model was developed with relatively large scales in mind, as BL development reflects surface conditions over scales of $\sim$10–100 km [*Andre et al.*, 1990; *Betts and Ball*, 1998]. The *Betts and Ball* [1998] model is consistent with the results of *Rabin et al.* [1990], who found that clouds formed first over wet areas when the atmosphere is relatively moist. However, *Rabin et al.* [1990] also reported that clouds formed first over areas with dry ground when the atmosphere is relatively dry.

[6] *Eltahir* [1998], also using FIFE data, proposed a mechanism to explain the soil moisture-rainfall feedback that was similar to *Betts and Ball* [1998] except it also focused on net radiation (R_n).

$$R_n = SW_n - LW_n = SW_d(1 - \alpha) + LW_d - LW_u \tag{2}$$

SW is shortwave radiation, LW is longwave radiation, α is surface albedo, and subscripts n, d and u refer to net, down and up. *Eltahir* [1998] hypothesized that high soil moisture increases the R_n absorbed at the land surface, thereby increasing Q_a and the moist static energy transported into the BL. The reverse would occur when the soil is dry. *Eltahir* [1998] proposed that the soil moisture-net radiation link was a key pathway in the soil moisture-rainfall feedback. Model simulations were consistent with this hypothesis [*Zheng and Eltahir*, 1998]. R_n is expected to increase when the soil is wet for several reasons: (1) the surface albedo is lower when soil is wet, increasing the net shortwave radiation; (2) wet soil increases EF, lowering the surface temperature and thereby decreasing the longwave radiation emitted by the surface; and (3) wet soil increases ET and water vapor in the atmosphere, increases downward longwave radiation via an enhanced local greenhouse effect. The first two feedbacks do not depend on a modification of BL conditions. Therefore these feedbacks can exist at small scales ($<\sim$1 km), and can be studied at the plot scale.

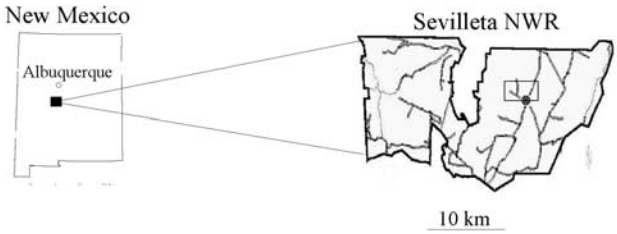

Figure 1. Location (small rectangle) of the shrubland and grassland field sites in the Sevilleta National Wildlife Refuge, central New Mexico. The city of Albuquerque is designated by the open circle.

[7] The total turbulent energy flux transferred into the BL from below (i.e., Q_a) is a key link between the land surface and the atmosphere [e.g., *Betts*, 2000]. It is critical to assess how R_n and Q_a depend on soil moisture because this dependence could lead to a feedback between soil moisture and rainfall. The results from the FIFE experiment were not conclusive. *Eltahir* [1998] found that daily-averaged R_n and Q_a were higher when the soil was wet, by $\sim$5% of the incident shortwave radiation. Using the same data, *Betts and Ball* [1998] reported that daytime G also increased when the soil was wet, offsetting any increases in R_n. Therefore the total energy transferred into the BL (Q_a) during the day did not depend on soil moisture.

[8] We focus on semiarid environments, where the connection between the land surface and the atmosphere is believed to be strong, and the surface radiation budget is expected to play an important role in the link [e.g., *Charney*, 1975; *Zheng and Eltahir*, 1998; *Small*, 2001]. We examine the relationship between soil moisture and the surface radiation budget, ground heat flux, and available energy in semiarid grassland and shrubland environments in central New Mexico (Figure 1), in order to test the various components of the soil moisture-net radiation feedback proposed by *Eltahir* [1998]. Figure 2 qualitatively shows that the soil moisture-R_n relationship proposed by *Eltahir* [1998] does exist in these environments: R_n is higher when the soil is relatively wet. Our goals are (1) to identify the processes that link variations in soil moisture, R_n, and Q_a; and (2) to provide quantitative estimates of the magnitude of the changes in energy balance resulting from soil moisture variations. The latter is critical to assess the importance of the proposed soil moisture-energy budget link, relative to other processes. In this paper, we do not assess how soil moisture influences evaporative fraction and BL conditions,

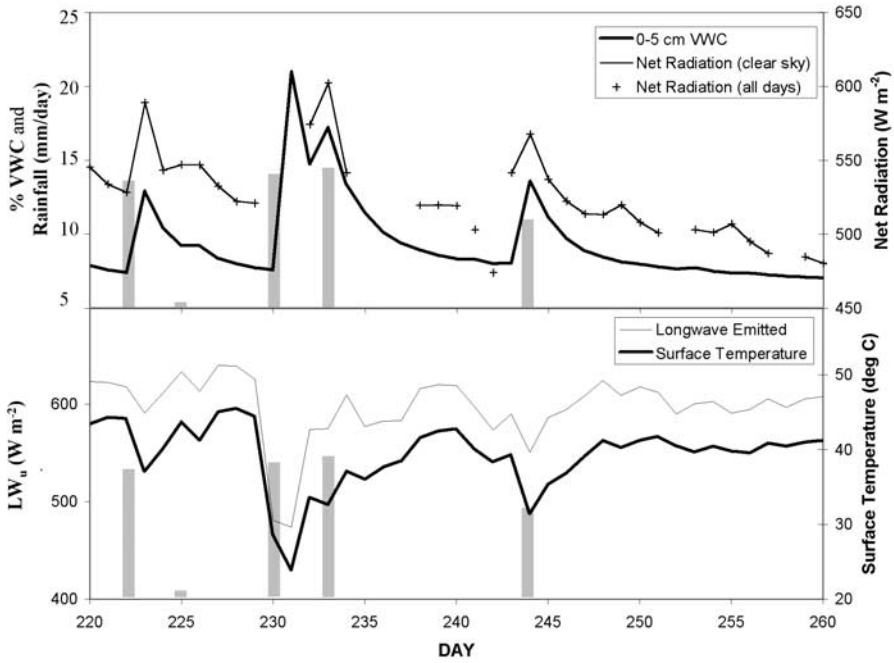

Figure 2. Time series from shrub site during 2001. (top) Rainfall (mm/day) and volumetric water content in the top 5 cm (θ_{0-5}) of the soil (left axis) and net radiation (right axis). Midday-averaged net radiation on all days is shown with pluses, and clear-sky net radiation days are shown by solid line. (bottom) Midday-averaged emitted longwave radiation (LW_u) and surface temperature.

although we intend to examine these relationships in future work. We describe the field sites, data sets, and analyses in section 2. Our results are described in section 3, followed by a discussion of how the soil moisture-R_n link described here may compare to that in other environments (section 4).

2. Study Area and Methods

2.1. Study Area

[9] We measured soil moisture and the components of the surface energy balance in grassland and shrubland ecosystems at the McKenzie Flats research area in the Sevilleta National Wildlife Refuge, central NM (Figure 1). The shrub and grass sites are only 2 km apart, as the grass-shrub ecotone is narrow at McKenzie Flats. The grassland site is dominated by Black Grama (*Bouteloua eriopoda*) grass and has ~50% canopy cover. The shrubland site is dominated by Creosotebush (*Larrea tridentata*) with only ~25% canopy cover. The vegetation is uniform around both sites for several hundred meters in all directions. The slope at both sites is <2 degrees. The surface soil is a sandy loam. The entire area has not been grazed since the 1970's.

[10] Annual precipitation is ~250 mm and more than half of the precipitation falls between July and September. Our analysis is restricted to the summers of 2000 and 2001. Figure 3 shows time series of precipitation, volumetric water content (θ) in the top 5 cm soil, and evapotranspiration (ET) during these intervals. Daily rainfall rarely exceeds 15 mm. The surface soil moisture increases following each rainfall event and typically dries before the next. On the daily timescale, the maximum surface (0–5 cm) θ is ~20% and the minimum is ~7%. During and soon after rainfall, instantaneous soil moisture values are as high as 30%, but these relatively wet conditions exist for only several hours. Following most rainfall events, the wetting front does not exceed 20 cm, with deeper infiltration occurring beneath plant canopies than beneath bare interspaces [*Bhark and Small*, 2003]. ET is measured at both sites using the Bowen Ratio method. These ET measurements have been compared against eddy correlation measurements at each site. The two methods yield similar ET time series, although the ET values from eddy correlation are usually lower by ~10%. ET varies with surface soil moisture: increasing after rainfall events and then decreasing to <1 mm day^{-1}. The EF is ~0.6 during the wet intervals and <0.1 during the dry intervals (not shown).

2.2. Data

[11] In this section, we introduce the data collected and instrumentation used. We also discuss how we calculate site-averaged values by combining measurements from bare soil and plant canopies. All radiation and surface variables were measured at 30 second intervals and then averaged and recorded every 30 minutes.

2.2.1. Radiation

[12] We measured the components of the surface radiation budget using identical radiometers at the two sites. Incident and reflected shortwave radiation were measured using Radiation and Energy Balance Systems (REBS) double-sided pyranometers. Downward and upward total radiation were measured using REBS total hemispheric radiometers (THRs). R_n was calculated from the difference between the downward and upward total radiation. Downward and upward longwave radiation were calculated by

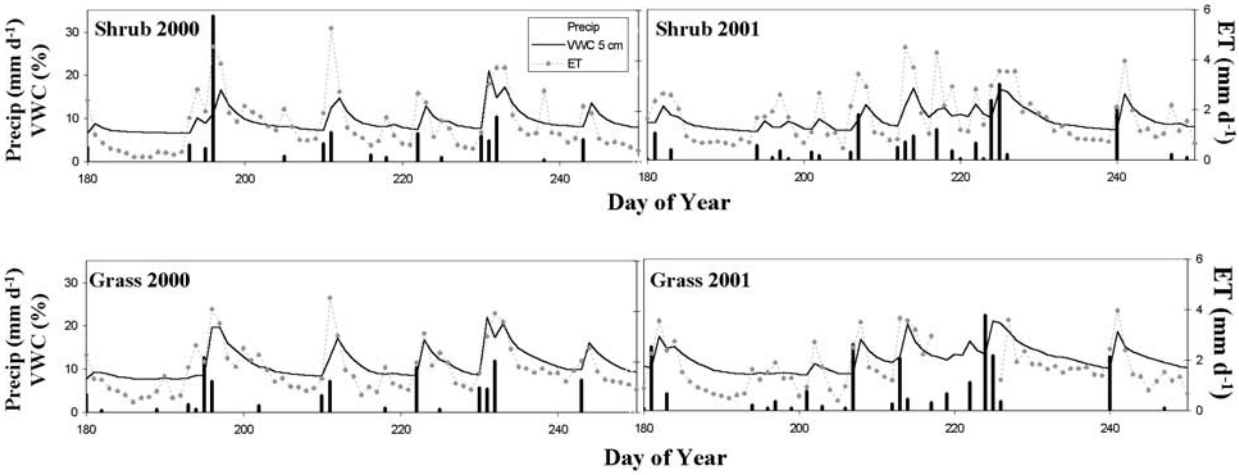

Figure 3. Time series of rainfall (vertical bars), θ_{0-5}, and ET at the shrub and grass sites during the 2000 and 2001 monsoon seasons (days 180–250). Precipitation and ET are daily average values. Water content is averaged between 10 AM and 3 PM. There is no ET data from the grass site 217–226 during 2001.

subtracting the measured shortwave radiation from the THR measurements (e.g., $LW_d = THR_d - SW_d$). All radiometers had built in ventilators, so corrections for variations in wind speed were not necessary. Prior to this study, we compared the radiometers in the field by setting them up side-by-side. Biases were less than 1% of midday values over a 5-day period, as reported in the instrument specifications. We also compared the R_n derived from the THRs with that from a REBS net radiometer, as used in studies such as FIFE [*Fritschen et al.*, 1992]. Again, values were within 1% of midday radiation values.

[13] The radiometers were placed 3.5 m above the soil surface, yielding a field of view for the downward facing radiometer with a radius of ~5 m. Therefore the measurements of upward radiation are averages over numerous plant canopies and interspaces, which is the primary source of heterogeneity in this environment. We completed net radiation surveys at each site to assess if the radiation measured at each tower is representative of the entire site. We compared the net radiation measured from the radiometers used in this study to synchronous measurements from a roving REBS net radiometer. R_n at the permanent site was within 2% of the value averaged over the surrounding 250m × 250 m areas. The grass site THR provided reliable measurements of R_n as demonstrated by our intercomparison. However, the partitioning between downward and upward total radiation was incorrect due to a wiring problem. We calculated LW_u at the grass site using net longwave from the grass site and downward longwave from the shrub site (i.e., $LW_u = LW_{net} - LW_{d\ shrub}$). The accuracy of LW_u at the grass site depends on the assumption that downward longwave radiation varies little over a horizontal distance of ~1 km, compared to variations in emitted longwave.

2.2.2. Ground Heat Flux and Soil Moisture

2.2.2.1. Subcanopy and Bare Ground Measurements

[14] In both environments, ground surface variables were measured beneath a plant canopy and the upslope, bare soil patch. These include ground heat flux, soil temperature, and soil moisture. We monitored canopy and interspace patches with dimensions that are typical of each environment. Site-averaged values were calculated by weighting the canopy and bare measurements by the percent cover of each. For example, the site-averaged VWC (θ) is

$$\theta = f\theta_c + (1 - f)\theta_b \tag{3}$$

where f is the fraction of canopy cover and subscripts c and b refer to canopy and bare. Both ground heat flux [*Kustas et al.*, 2000] and soil moisture [*Bhark and Small*, 2003] exhibit substantial differences between canopy and bare patches in environments with sparse vegetation. Our weighting strategy (equation 3) controls for the spatial variability resulting from vegetation, which is the primary source of soil moisture variability in this environment.

2.2.2.2. Ground Heat Flux and Soil Temperature

[15] The ground heat flux was measured using a combined calorimetric-heat flux plate approach [*Kimball et al.*, 1976]. The heat flux from the soil surface to 5 cm depth was calculated from the change in temperature averaged over this depth interval, measured with an averaging thermocouple. The specific heat of the soil was adjusted at each time based on the measured volumetric water content. REBS ground heat flux plates were placed at a soil depth of 5 cm. We did not adjust the soil heat flux plate measurement for contrasts in thermal conductivity between the plate and soil. The adjustments for focused heat flow through a disk with a different thermal conductivity [*Turcotte and Shubert*, 1982] were always less than several W m^{-2}.

2.2.2.3. Soil Moisture

[16] Soil moisture profiles were monitored at the same canopy and bare soil locations where heat flux and soil temperature were measured. Campbell Scientific water content reflectometers (WCR) were inserted at three depths: 2.5, 12.5, and 22.5 cm. The probes provide estimates of volumetric water content based on the time domain reflectometry method (TDR) [*Topp et al.*, 1980]. Probes were inserted horizontally in the upslope direction from a shallow pit that was subsequently filled. The WRCs have two 30 cm rods spaced 3.2 cm apart. A probe with this geometry

samples a semi-cyclindrical region around the rods. 90% of the signal is derived from soil between 2.5 cm above and below the rods [*Ferre et al.*, 1998]. Therefore the probe inserted at 2.5 cm provides an estimate of VWC in the top 5 cm of soil. We use the factory calibration for the WCRs, which was completed using low-salinity, sandy soils like those in our study area. The WCR values are consistent with synchronous, nearby gravimetric and TDR estimates of soil moisture.

[17] The surface soil moisture time series at each site are calculated from only two probes (canopy and bare soil). We have checked to make sure that these site-averaged time series are representative by comparing them to concurrent measurements of soil moisture from a TDR array that includes 9 probes. The 9 probes were also placed at a depth of 2.5 cm and averaged over canopy and bare soil according to equation 3. The TDR probe array is located ~1 km from both sites studied here and recorded data continuously for 60 days, including 3 rainfall events and subsequent dry downs. The site-averaged time series (from 2 probes) are highly correlated with the time series from 9 probes: r^2 values are 0.90 and 0.86 from the grass and shrub sites, respectively. The grassland and shrubland soil moisture time series are also highly correlated ($r^2 = 0.86$, Figure 3). This comparison shows that the soil moisture time series used in our analyses do represent the temporal variability of soil moisture in the study area. In comparison, the correlation between canopy and bare soil moisture time series, recorded at probes only 1 m apart, is somewhat lower ($r^2 = 0.70$).

2.3. Data Analysis

2.3.1. Period of Record

[18] Data were recorded continuously from May–October in 2000 and 2001. The THR at the grass site did not provide reliable data after day of year (DOY) 225 in 2001 because the THR dome cracked and the instrument got wet. The R_n measurements following this incident are unreliable. Therefore we exclude data from both sites that was collected after this date to provide an unbiased comparison between the two environments.

2.3.2. Other Sources of Variability

[19] Our goal is to investigate how the surface radiation budget and ground heat flux vary with soil moisture in order to test hypotheses concerning the nature of land-atmosphere interactions [e.g., *Eltahir*, 1998; *Betts and Ball*, 1998]. In addition to identifying key linkages, we also want to generate quantitative estimate of the magnitude of the changes in energy balance resulting from soil moisture variations. The main challenge we faced is that the surface radiation budget and ground heat flux are influenced by more than just soil moisture. Two important factors that influence the surface energy budget, through variations in incident shortwave radiation and other variables, are the seasonal cycle and clouds. We now outline how we control for the effects of these factors on the relationship between the energy budget and soil moisture.

2.3.3. Seasonal Cycle

[20] Clear-sky incident shortwave radiation varies by ~20% between June and October, as do other components of the surface radiation budget. The temporal evolution of the surface soil moisture field is tightly linked to the seasonal cycle in our study area. The soil is typically dry in May and June prior to the onset of the North American monsoon [*Higgins et al.*, 1998]. In July through September, the soil is repeatedly wetted and dried (Figures 3, 4a, and 4b). Therefore the radiation budget-soil moisture relationship would be modified by the seasonal cycle of radiation if we included data from May or June in our analysis. For example, it would appear that incident shortwave radiation, and therefore net shortwave radiation, was higher when soil moisture was dry, only because the soil is nearly always dry in June when the incident shortwave radiation is highest. One strategy for minimizing the influence of the seasonal cycle is to normalize all variables by the time series of incident shortwave radiation, as done by *Eltahir* [1998]. However, various elements of the surface energy balance exhibit noticeable seasonal cycles even after they have been normalized by incident shortwave radiation (Figures 4d and 4f). This is clearly not a viable solution in the environment examined here.

[21] We only use data between DOY 180 and 250 (1 July to 10 September) to minimize the effects of the seasonal cycle. There are two benefits to this approach. First, seasonally-driven radiation variations are not large over this interval (Figures 4c–4f). Second, temporal variations of soil moisture are not linked to the seasonal cycle during this interval (Figures 4a and 4b). Instead, the surface soil moisture variations reflect rainfall events and subsequent dry downs. In addition, this is the period when convective rainstorms are common, so it is the most relevant for discussions of land-atmosphere interactions. Excluding days with radiometer problems, this leaves 120 days for analysis.

2.3.4. Clouds

[22] Clouds have a larger influence on the surface radiation budget than do seasonal variations (Figure 4). We completed our analyses for two sets of the data: clear-sky only and all days. Each day in the record was designated clear-sky (or not) if the midday incident shortwave radiation was within 10% of highest values observed during that time of the year. The total number of clear-sky days is 81, after including only days within seasonal cutoffs and days with complete data. Analysis of the clear-sky subset makes it easier to identify links between soil moisture and the surface radiation budget, by minimizing the noise associated with cloudiness. However, analysis of all days provides a more complete picture of the links between soil moisture and SEB variations, as a positive covariance may exist between soil moisture and cloudiness.

2.3.5. Daily Averaging Period

[23] Diurnal cycles of surface energy balance variables and temperature are displayed in Figure 5. Except where noted otherwise, we used average values from 10 AM to 3 PM in our analyses. We selected this averaging period because it is centered around the daily Q_a maximum (Figure 5), when the influence of the land surface on BL conditions is strongest. We completed all analyses for different averaging periods and found similar results.

2.3.6. Wet and Dry Composites

[24] We processed the data in two ways. First, we used the days with the highest and lowest soil moisture to construct wet and dry composites, similar to the wet and dry end-members used in the FIFE study [*Eltahir*, 1998; *Betts and Ball*, 1998]. We included roughly one third of the data in each end-member, which required using a different

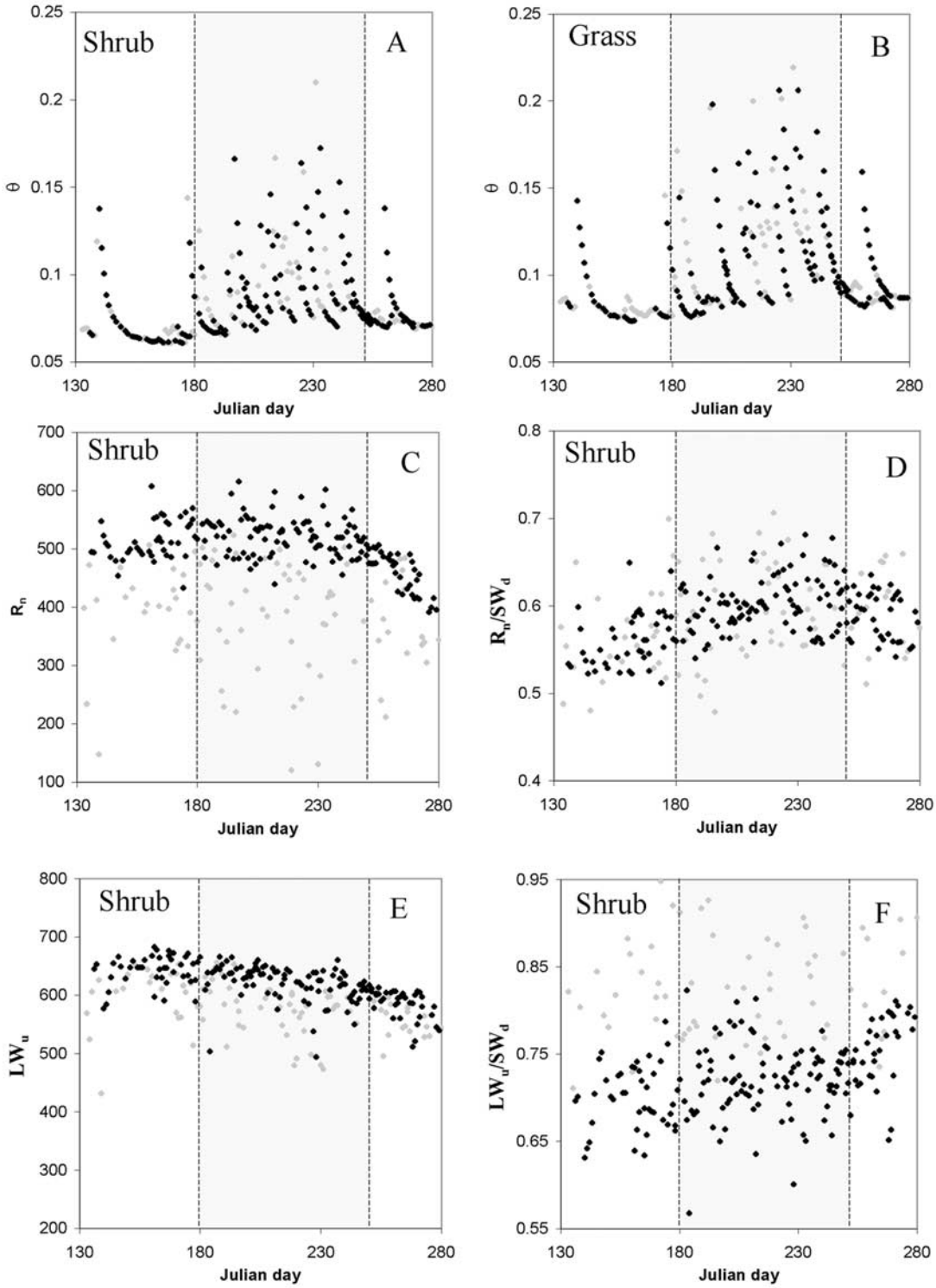

Figure 4. Seasonal cycles (2000 and 2001) of θ_{0-5} from the (a) shrub and (b) grass sites and various components of the radiation budget from the shrub site, including (c) net radiation; (d) net radiation normalized by incident shortwave radiation; (e) emitted longwave radiation; and (f) emitted longwave radiation normalized by incident shortwave radiation. The solid points are data from clear sky days and the shaded points are from other days. Data from 2000 and 2001 are combined on these plots. All points are averages between 10 AM and 3 PM. The region between the dashed lines shows the analysis period used here (day of year 180–250).

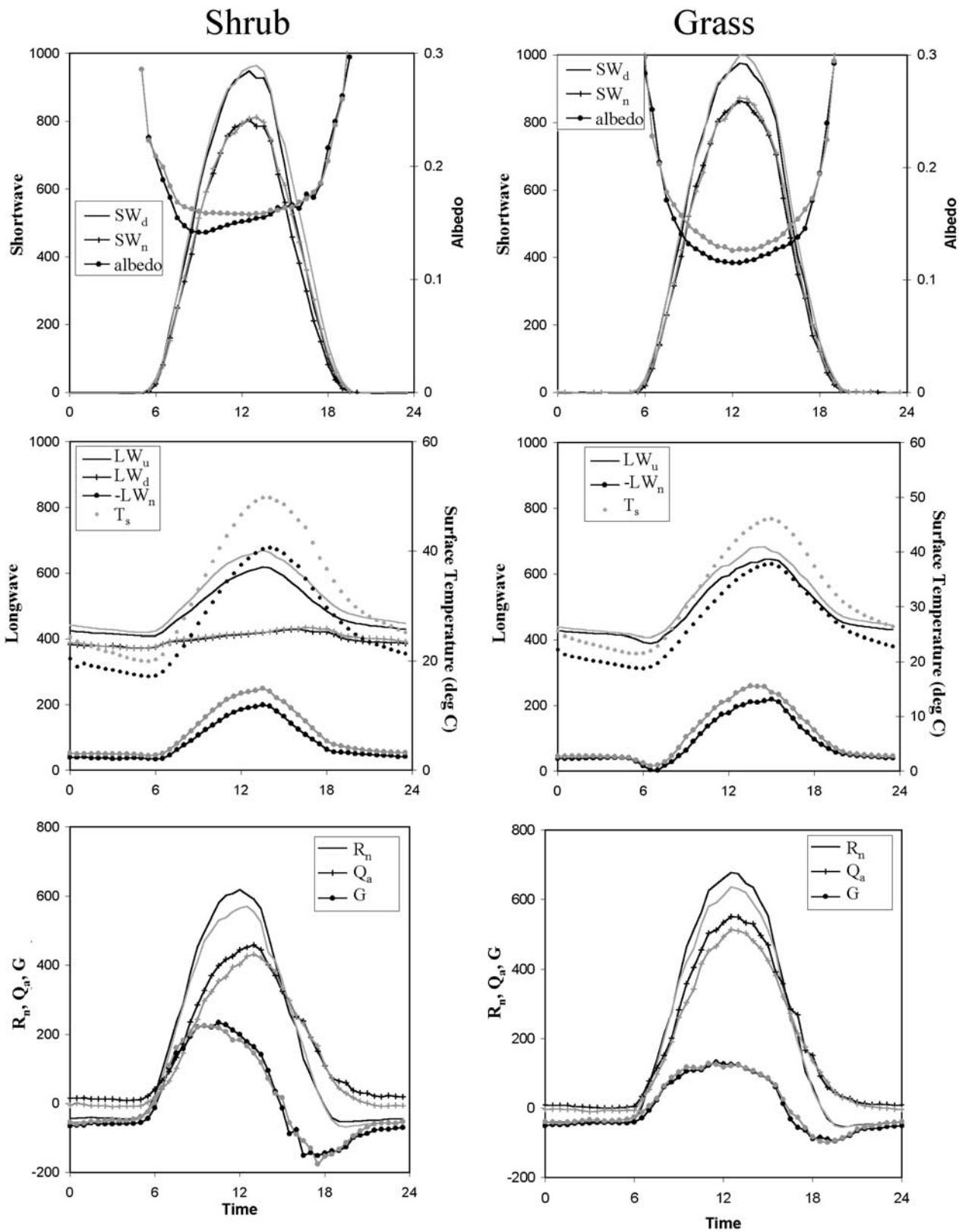

Figure 5. Average diurnal cycles for clear-sky days from the wet (solid lines and symbols) and dry (shaded lines and symbols) soil moisture composites at the shrub (left) and grass (right) sites. (top) Shortwave down, net shortwave radiation, and albedo. (middle) Longwave radiation (up, down, and net) and surface temperature. The net values longwave values are multiplied by -1. Longwave down is not measured at grass site. (bottom) Net radiation, available energy, and ground heat flux. Units are W m^{-2}, except for surface temperature (°C) and albedo.

Table 1. Mean Values of Volumetric Water Content (θ), Threshold Values Used to Identify Wet and Dry Days (θ Cutoff), Surface Radiation Budget Components, Ground Heat Flux, and Surface Temperature (Average, Subcanopy, and Bare) for the Wettest and Driest Midsummer, Clear-Sky Days[a]

	Shrub			Grass		
	Wet	Dry	Wet-Dry	Wet	Dry	Wet-Dry
n	14	23		16	20	
θ (%)	13.4	7.2	6.2	16.1	8.5	7.6
θ cutoff (%)	>.11	<0.09		>.125	<0.09	
SW_n	743	747	−4	805	809	−4
SW_d	877	887	−10	913	929	−16
Albedo (%)	15.2	15.7	−0.5	11.8	12.9	−1.1
LW_n	−180	−221	41	−178	−223	46
LW_d	416	417	−1	420	421	0
LW_u	596	638	−42	598	644	−46
R_n	563	527	36	618	578	39
G	150	141	9	110	110	0
Q_a	413	386	26	508	469	39
T_{avg}	37	45	−8	35	42	−7
T_b	42	50	−9	42	50	−7
T_c	26	33	−7	27	34	−7

[a]The difference between wet and dry values are shown. Values are averaged between 10 AM and 3 PM. All surface energy balance components are in W m^{-2}.

Table 2. Mean Values of Volumetric Water Content (θ), Surface Radiation Budget Components, Ground Heat Flux, and Surface Temperature (Average, Subcanopy, and Bare) for the Wettest and Driest Midsummer Days[a]

	Shrub			Grass		
	Wet	Dry	Wet-Dry	Wet	Dry	Wet-Dry
n	25	41		34	40	
θ (%)	13.2	7.2	6.0	15.5	8.4	7.1
SW_n	656	667	−12	702	723	−21
SW_d	770	790	−20	800	830	−30
Albedo (%)	14.6	15.5	−0.9	12.3	12.9	−0.6
LW_n	−158	−197	40	−158	−198	40
LW_d	423	426	−3	424	423	0
LW_u	581	623	−42	582	620	−39
R_n	493	463	30	534	515	19
G	112	105	7	90	89	2
Q_a	381	358	23	443	426	17
T_{surf}	35	44	−9	34	40	−7
T_b	40	49	−9	40	47	−7
T_c	26	33	−7	27	34	−6

[a]The difference between wet and dry values are shown. Values are averaged between 10 AM and 3 PM. Wet and dry day cutoff values same as for clear-sky days (Table 1). All surface energy balance components are in W m^{-2}.

cutoff value for wet days at the two sites (Table 1). The average soil moisture difference between the composites is ∼7% VWC, compared to the full range observed of ∼15%. Tables 1 and 2 show midday averages for the wet and dry composites, from clear and all-days, respectively. This analysis is based on arbitrarily chosen cutoffs for dry and wet soil. The magnitudes and statistical significance of wet-dry differences depend on the chosen cutoff values. Therefore we accompany the wet-dry composites with regression analyses that incorporate data from all days.

2.3.7. Slope Estimates

[25] Second, we estimated the slope of different SEB components and surface temperature with respect to soil moisture. The calculated slope values were then scaled to the range of midday-averaged VWC observed, ∼15% in both environments. These values are reported in Table 3. For example, the change in net radiation, ΔR_n, over the observed range in soil moisture was calculated as

$$\Delta R_n = \frac{dR_n}{d\theta}(\theta_{max} - \theta_{min}) = \frac{dR_n}{d\theta}0.15 \quad (4)$$

[26] The regression analysis is based on the assumption that the relationship between surface energy balance components and soil moisture is linear. The linear assumption appears to be more reasonable for some SEB components than others (discussed below). We calculate error estimates on the calculated slope (ε) as $\varepsilon = t(\alpha/2, df_{n-2})S_b$, where t is the critical t-value for some significance level (α) and degrees of freedom (df), and S_b is the standard error of the slope. N is the number of daily-averaged values in the data records, 81 for the clear-sky data. All calculations were completed for α = 99%. The error estimates for the slope are also scaled to the range of VWC observed.

[27] The range of midday averaged VWC is ∼15% in both environments, from 7–22%. In comparison, the range of instantaneous VWC is greater (∼25%), so using the midday values provides a conservative estimate of the range of variations in SEB components related to soil moisture variations. It is not possible to evaluate the influence of the wettest soil moisture conditions, which occur during or soon after rainfall events, on the surface radiation budget, ground heat flux, and surface temperature. This would require using 30-minute averaged values instead of midday averages, introducing the complexity of comparing observations from different times within the daily cycle.

3. Results

[28] In this section, we describe how the different elements of the surface radiation budget, ground heat flux, and available energy vary as a function of soil moisture. This is done in two different ways: (1) comparing the ensembles from dry and wet soil moisture conditions; and (2) assessing

Table 3. Changes (Wet Minus Dry) in Surface Radiation Budget Components, Ground Heat Flux, and Surface Temperature Estimated From Linear Regression Versus Surface Volumetric Water Content (0–5 cm)[a]

	Clear Sky		All Days	
	Shrub	Grass	Shrub	Grass
SW_{net}	7 ± 39	5 ± 34	−48 ± 136	−13 ± 113
SW_{in}	−8 ± 51	−9 ± 47	−77 ± 162	−28 ± 129
Albedo (%)	**1.5 ± 1.4**	**1.4 ± 1.2**	**3.1 ± 1.01**	**1.5 ± 0.9**
LW_n	**97 ± 23**	**81 ± 23**	**98 ± 40**	**74 ± 33**
LW_d	−2 ± 19	NA	−8 ± 19	NA
LW_u	**−99 ± 26**	**−85 ± 22**	**−107 ± 40**	**−75 ± 32**
R_n	**104 ± 31**	**83 ± 25**	54 ± 104	65 ± 84
G	23 ± 36	7 ± 13	8 ± 64	10 ± 28
Q_a	**81 ± 36**	**76 ± 25**	50 ± 66	55 ± 64
T_{surf}	**−20 ± 4**	**−14 ± 3**	**−21 ± 4**	**−13 ± 3**
LW_u (predicted)	**−132 ± 26**	**−88 ± 14**	**−135 ± 28**	**−82 ± 18**

[a]Slope and slope error from regression are scaled over the range of soil moisture observed (15%) (equation 3). Changes that are significant at the 99% confidence interval are in bold. All surface energy balance components are in W m^{-2}.

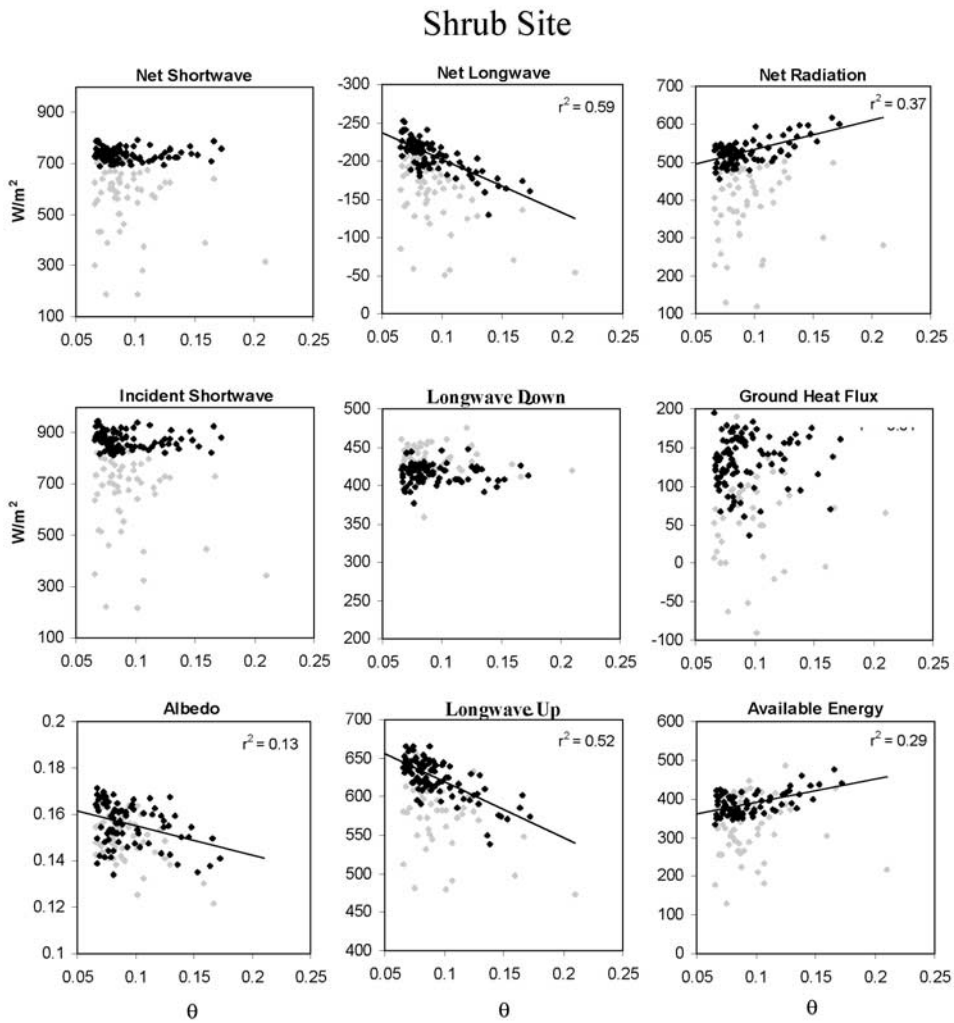

Figure 6. Relationship between soil moisture and different components of the surface radiation budget and ground heat flux at the shrub site, for both 2000 and 2001. Y axis units are W/m^2 except for plot of albedo (unitless). X axis on all plots (θ) is volumetric water content in the top 5 cm of the soil. Each point represents a different day, with values averaged over the interval 10 AM to 3 PM. Solid points are from clear sky days, and shaded points are from other days. Least squares linear fit to clear sky points and r^2 values are shown, except when r^2 is <= 0.01.

how each field varies as a function of soil water content (regression analysis). The data from clear-sky days is discussed first (sections 3.1–3.5). Then, all the data is used to assess the influence of clouds (section 3.6).

3.1. Shortwave Radiation and Albedo

[29] The surface albedo is lower when the soil is wet at both the grass and shrub sites (Figure 5). The midday-averaged albedo difference between wet and dry composites is 1.1% at the grass site and 0.5% at the shrub site (Table 1). Even though the albedo is lower when the soil is wet, the observed differences in net shortwave radiation are very small (<5 W m^{-2}) at both sites (Figure 5 and Table 1). Incident shortwave radiation is lower by 10–15 W m^{-2} when the soil is wet (Table 1). This offsets any increase in net shortwave that could result from the lower albedo of wet soils.

[30] The regression analysis yields a similar result. There is a significant trend between albedo and VWC at both sites (Figures 6 and 7 and Table 3), but there is substantial scatter around the best fit line. Albedo decreases by ~1.5% over the range of soil moisture observed (15% VWC), calculated according to equation 4. There is no trend between net or incident shortwave and VWC (Figures 6 and 7 and Table 3). We conclude that changes in net shortwave radiation are negligible. The decrease in albedo with wet soil is too small to have a measurable influence given the observed variability of shortwave radiation. An experiment that minimizes the effects of day-to-day variability by comparing paired wet and dry plots is necessary to assess if an important relationship exists between soil moisture and net shortwave radiation.

3.2. Longwave Radiation

[31] At both sites, the longwave radiation emitted (LW_u) by the surface is lower throughout the entire day when the soil is wet (Figure 5). The difference in emitted longwave radiation between wet and dry conditions is greatest during

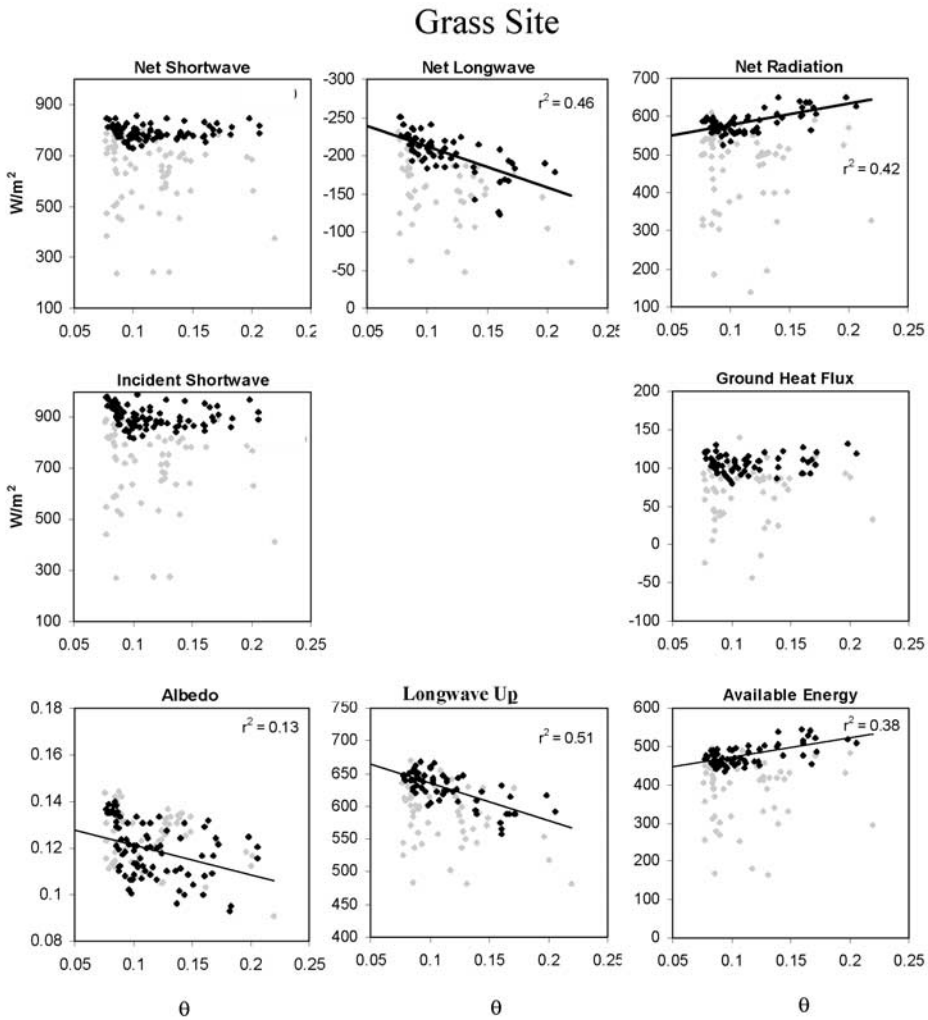

Figure 7. Same as Figure 6 except from the grass site.

the middle of the day, -45 W m^{-2} at both sites (Table 1). The downward longwave radiation is nearly identical under dry and wet soil moisture conditions at the shrub site (Figure 5 and Table 1). Downward longwave radiation was not measured at the grass site. The observed difference in net longwave radiation between dry and wet soil composites is 45 W m^{-2} averaged throughout the midday interval, equal in magnitude but opposite in sign to the changes in emitted longwave radiation.

[32] The regression analysis yields a similar result. Downward longwave radiation is not correlated with surface soil moisture (Figures 6 and Table 3). In contrast, both net and emitted longwave radiation are clearly correlated with soil moisture. From the driest to the wettest soil conditions, emitted longwave radiation decreases by 99 ± 26 W m^{-2} at the shrub site and 85 ± 22 W m^{-2} at the grass site. The changes in net longwave are of the same magnitude but are opposite in sign.

3.3. Surface Temperature

[33] The midday surface temperature (0–5 cm) in the wet soil composite is 7–8°C cooler than in the dry composite (Table 1), for both subcanopy and bare soil. Two processes contribute to these temperature variations. First, and probably most important, ET is high when the soil is wet (Figure 3). ET varies linearly with 5 cm soil moisture, with r^2 values exceeding 0.8 [*Small and Kurc*, 2001]. High ET results in relatively low Bowen ratios and surface temperatures. Second, the specific heat of the soil increases by ~40% for a 15% VWC increase, slowing the heating rate during the morning hours.

[34] Figure 8 shows scatterplots of surface soil temperature versus soil moisture, including plots for bare, subcanopy, and average soil. In all cases, soil temperature decreases significantly with increasing water content. Surface temperature decreases by 20 ± 4°C at the shrub site and 14 ± 3°C at the grass site over the range of soil moisture observed (Table 3). The r^2 values are higher than for the radiation fields (Figure 6). However, the linear model does not provide a perfect fit to the data, particularly at the shrub site.

[35] We estimate the emitted longwave radiation using the Stefan-Boltzmann law ($\varepsilon = 0.95$) from the 30-minute surface temperature data. This calculation was completed separately for canopy and bare soil, and then weighted according to equation 3. Then, we calculated midday values of the predicted emitted longwave radiation (10 AM to 3 PM) and completed a regression against soil moisture.

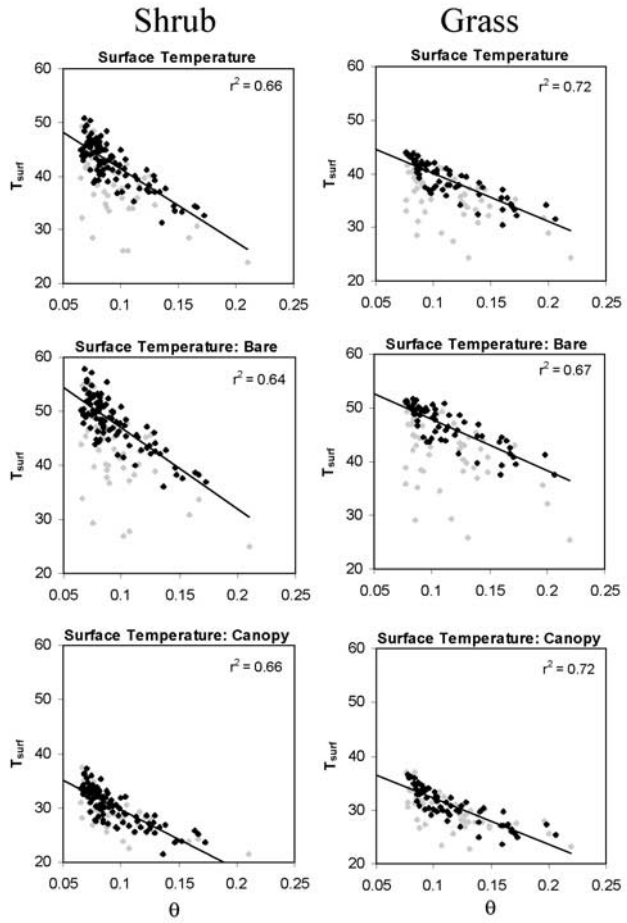

Figure 8. Relationship between soil volumetric water content (θ_{0-5}) and surface temperature averaged over the top 5 cm of the soil. Solid points are from clear sky days, and shaded points are from other days, from 2000 and 2001. Least squares linear fit to clear sky points and r^2 values are shown. (top) Average surface temperature. (middle) Surface temperature from bare soil area. (bottom) Surface temperature beneath plant canopy.

The predicted decrease in emitted longwave radiation derived from the surface temperature measurements closely matches the measured decrease in emitted longwave at the grass site (Table 3). At the shrub site, the predicted decrease is too high by ~30%, perhaps reflecting the greater vertical separation between the soil and canopy in this environment. In both cases, the close correspondence between the measured and estimated variations of longwave radiation with soil moisture shows that the temperature and radiation data are physically consistent.

3.4. Ground Heat Flux

[36] The differences in site-averaged ground heat flux between wet and dry soils are small compared to the observed differences in longwave radiation (Table 1). At the shrub site, the wet soil ground heat flux is 10 W m^{-2} higher than the dry soil ground heat flux. The wet and dry soil ground heat flux values are the same at the grass site. There is no correlation between ground heat flux and soil moisture at either site (Table 3 and Figures 6 and 7). Given the substantial scatter between G and θ at the shrub site (Figure 6), we expect that the wet-dry G difference (Table 1) observed at the shrub site reflects noise rather than a real trend.

[37] The measured ground heat flux does not vary significantly with soil moisture because soil moisture-induced changes in the vertical temperature gradient and thermal conductivity are opposite in sign. The thermal conductivity of the soil, k, is higher when soil is wet. We estimated variations in k driven by the observed fluctuations in soil moisture and temperature using the method described by *Campbell and Norman* [1998]. The estimated k values are ~40–60% higher on the days in the wet soil composite. We do not directly measure the temperature gradient at the depth of the soil heat flux plates (5 cm). However, we do measure soil temperature at depths of 2.5 and 12.5 cm. The midday vertical temperature gradient between these depths is lower by ~50% in the wet soil composites. The change in the vertical temperature gradient is the result of the substantial decreases in surface soil temperature when the soil is wet (Figure 8).

3.5. Net Radiation and Available Energy

[38] Midday net radiation is 35–40 W m^{-2} higher in the wet composites than in the dry composites (Table 1). This difference is the result of the change in net longwave radiation because net shortwave does not vary with soil moisture ($\Delta R_n = \Delta SW_n + \Delta LW_n$). The greatest differences in R_n exist between 9 AM and 3 PM, when the wet-dry temperature and net longwave contrasts are most extreme (Figure 5). R_n clearly increases with water content over the entire range of soil moisture observed (Figures 6 and 7 and Table 3). The slope of the regression is similar at the two sites. R_n increases by 104 ± 31 and 83 ± 25 W m^{-2} at the shrub and grass sites, respectively, over a surface soil moisture range of 15%. This increase is equal to ~20% of the dry value of R_n.

[39] At the grass site, the difference between available energy (Q_a) in the wet and dry soil composites is nearly identical to the R_n differences (Table 1 and Figure 5). This is expected given that ground heat flux does not vary with soil moisture in this environment. The wet-dry differences in Q_a are slightly reduced relative to the R_n differences at the shrub site, where the site-averaged ground heat flux is slightly higher in the wet soil composite. The regression analysis shows that Q_a clearly increases over the entire range of observed water contents (Figure 6). The increase is ~80 W m^{-2} at both sites, equal to ~20% of Q_a in these semiarid environments.

3.6. Effects of Clouds

[40] Variations in incident shortwave radiation caused by clouds influence all other components of the radiation budget, ground heat flux, and surface temperature. The variations in other surface variables do not scale proportionally with fluctuations in incident shortwave (Figures 4d and 4f). Therefore normalizing all variables by SW_d does not eliminate the effects of clouds. Effectively, clouds introduce noise into the analysis (Figures 6 and 7). When all days are considered, significant correlations with soil moisture only exist for longwave radiation (net and up), albedo, and surface temperature (Table 3). Significant correlations with net radiation and available energy do not

exist when all days are considered, unlike the result derived from the clear-sky analysis.

[41] The relationship between longwave radiation and soil moisture fluctuations are nearly identical when either clear-sky or all days are considered, based on both the wet-dry composite differences and regressions analyses. Considering all days, net longwave is ~40 W m^{-2} higher in the wet soil composite (Table 2). Emitted longwave decreases by a similar amount and the wet-dry difference in LW_d is negligible. Over the observed range in soil moisture, net longwave increases by 107 ± 40 and 75 ± 32 W m^{-2} at the shrub and grass sites, respectively. The relationship between surface temperature and soil moisture is very similar for clear-sky and all days (Table 3). Therefore it is expected that the soil moisture-induced longwave radiation fluctuations are similar when either clear-sky or all days are considered.

[42] The albedo variations are also similar between clear-sky and all days (Tables 2 and 3). When all days are considered, both SW_d and SW_{net} are lower by 10–30 W m^{-2} in the wet composites. This SW decrease with wet soil is twice as large as that observed on clear-sky days (Table 1). There is no significant correlation between either SW component and soil moisture (Table 3 and Figures 5 and 6), so the lower SW_{net} values observed when the soil is wet could simply reflect noise. However, the lower SW_{net} under wet soil conditions influences the soil moisture-R_n relationship. The wet-dry R_n differences are not as large when cloudy days are included, particularly at the grass site where the wet-dry difference decreases by half (40 to 20 W m^{-2}) (Table 2). Variations in G with soil moisture are the same for clear-sky and all days. So, the variations of Q_a with soil moisture are roughly equal to the variations in R_n when all days are included.

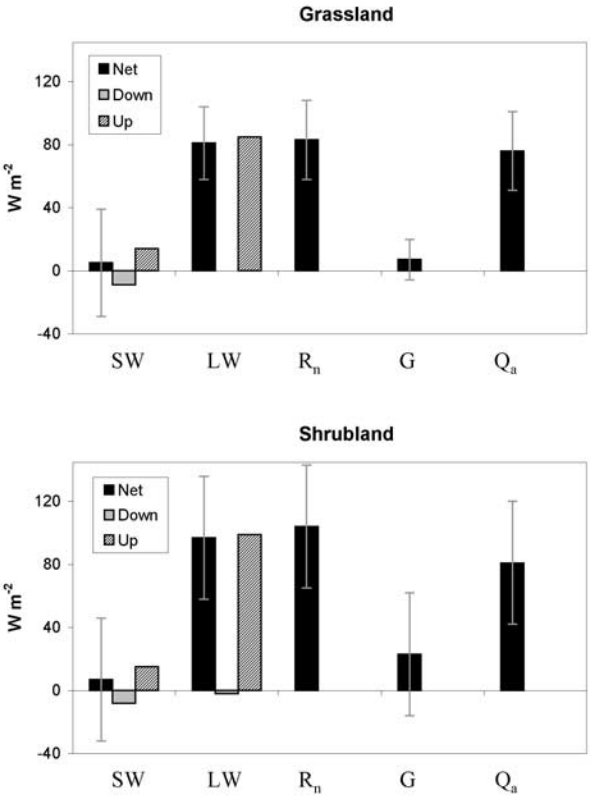

Figure 9. Summary of surface radiation and energy budget changes (wet minus dry) associated with a surface volumetric water content increase of 15% at the grassland and shrubland sites. Error bars show 99% confidence interval estimates determined from regression analysis, only shown for net values. Downward longwave radiation data were not reliable at grassland site, so they are not included.

4. Discussion

[43] The data presented above provides a clear picture of how soil moisture variations influence the surface radiation balance, ground heat flux, and available energy in two different semiarid ecosystems. These relationships for clear-sky conditions are summarized in Figure 9. The changes are based on the slope estimates from the regression analysis scaled over the observed water content variations (15%). The soil temperature decreases by >10°C when the surface soil is wet. This results in a large and statistically significant decrease (~85–100 W m^{-2}) in longwave radiation emitted at the surface, a positive contribution to the surface radiation budget. Downward longwave radiation does not vary with soil moisture. Therefore changes in net longwave radiation equal the changes in emitted longwave radiation. The observed changes in net shortwave radiation are small in comparison (<10 W m^{-2}) and are not statistically significant. The surface albedo decreases by ~1.5%, decreasing the shortwave radiation reflected by the surface by only ~10 W m^{-2}. Net radiation increases by an amount roughly equal to the decrease in emitted longwave radiation (85–100 W m^{-2}). Changes in ground heat flux are negligible at the grass site. The ground heat flux may be slightly higher when the soil is wet at the shrub site, but this cannot be confirmed with our data. The available energy is higher by 80 W m^{-2} at both sites when the soil is wet, again primarily a result of the decrease in longwave radiation emitted by the surface. This change is 22% of average Q_a at the shrub site and 19% at the grass site. The percent change is smaller at the grass site because available energy is higher in this environment, due to lower albedo and midday G.

[44] Our results suggest that the model proposed by *Eltahir* [1998] partially describes the key links between soil moisture and net radiation or available energy in semiarid environments. However, some of the details of the model do not apply. First, *Eltahir* [1998] proposed that downward longwave radiation should increase with soil moisture because enhanced ET increases the concentration of atmospheric water vapor. Downward longwave radiation data was not reliable from the grassland site, so our grassland data does not confirm or refute this hypothesis. However, data from the shrubland site clearly shows that there is no relationship between soil moisture and downward longwave radiation, perhaps because rainfall and the associated soil moisture anomalies are patchy relative to the lengthscale over which the BL develops. Second, although albedo is higher when the soil is wet, changes in net shortwave radiation are minor. And third, changes in ground heat flux may be important, as suggested by *Betts and Ball* [1998]. Spatially-distributed monitoring of ground heat flux [e.g., *Kustas et al.*, 2000] is necessary to assess the temporal covariance between ground heat flux and soil moisture.

[45] The observed soil moisture-induced Q_a variations are large (80 W m^{-2} or 20%) compared to other sources of spatial and temporal variability in Q_a. First, the soil moisture-induced variations described here are as large or larger than spatial variations in Q_a across various midlatitude environments. Midday Q_a in the semiarid Sevilleta grassland is 55 W m^{-2} higher than in the adjacent shrubland. Midday Q_a in the Konza prairie grassland, the location of FIFE, is 10 W m^{-2} higher than the Sevilleta grassland [*Betts and Ball*, 1998]. Summertime midday Q_a at the Duke Forest is ~450 W m^{-2} [*Katul et al.*, 2001] (see http://www.env.duke.edu/other/AMERIFLUX/amerflux.html), 85 and 30 W m^{-2} higher than the Sevilleta shrubland and grassland, respectively. Second, the soil moisture-induced Q_a variations are of similar magnitude to Q_a changes related to natural or human-induced land cover change. Simulated and observed Amazonian deforestation lowers R_n by ~15% [*Gash and Nobre*, 1997; *Lean and Warrilow*, 1989; *Shukla et al.*, 1990], and Q_a would be slightly larger given reasonable increases in G. Land surface changes in semiarid regions are often discussed with regard to changes in albedo, varying from ~20% [e.g., *Charney*, 1975] to only several percent [e.g., *Grover and Musick*, 1990]. The former yields midday Q_a changes of ~100 W m^{-2}. Third, the soil moisture-driven Q_a variations are roughly half as large as the Q_a variations resulting from the seasonal cycle and cloud cover (Figures 6 and 7), both which are ~150 W m^{-2}.

[46] Do variations in Q_a as large as 80 W m^{-2} influence boundary layer characteristics and convective precipitation? A 20% increase in Q_a would increase the rate that moist static energy is transferred into the boundary layer by 20%, if variations in Q_a do not directly influence boundary layer depth or diabatic heating [e.g., *Betts*, 2000]. In our study area, high soil moisture raises the evaporative fraction, lowers the surface temperature, and increases net radiation. Because Q_a and EF positively covary, the enhanced surface-to-boundary layer flux of energy should be accompanied by a decrease in BL depth [*Betts*, 2000]. Results from previous modeling studies suggest Q_a variations discussed here are large enough to have a substantial impact. Many modeling studies have demonstrated that ~15% changes in R_n, when combined with other land surface changes, yield substantial climatic impacts [e.g., *Lean and Warrilow*, 1989]. *Zheng and Eltahir* [1998] used a zonally-symmetric model to isolate the effects of soil moisture-induced net radiation anomalies on subsequent rainfall in West Africa. They found that a net radiation change of only ~30 W m^{-2} (daily average) substantially enhanced the magnitude and persistence of wet conditions, relative to the effects of ET changes alone.

[47] The magnitude of soil moisture-induced fluctuations of R_n and Q_a is large. However, the intervals during which soil moisture is high, and therefore R_n and Q_a are enhanced, are short. The surface soil moisture is only high for several days after rainfall events (Figures 2 and 3). After roughly 1 week, the surface soil moisture typically decreases to the pre-storm value (~8% VWC). During the summer, soil moisture at deeper levels follows similar patterns to that at the surface, although the post-rainfall rise and subsequent dry down are typically of smaller amplitude and are less rapid. ET, surface temperature, R_n and LW_u vary with surface soil moisture, so their rainfall-induced anomalies are similarly of short duration (Figures 3). The soil moisture-R_n relationship documented here can only contribute to a soil moisture-rainfall feedback if enhanced land-atmosphere turbulent energy transfer exists during periods when atmospheric conditions promote convective rainfall. As the duration of R_n anomalies is short in semiarid environments, the influence of soil moisture on future rainfall via the effects on the surface radiation budget may be negligible. Investigating the temporal covariance of R_n anomalies and synoptic-scale atmospheric conditions is an avenue for future research.

[48] The influence of soil moisture on R_n and Q_a appears to be much stronger in the semiarid environments studied here than in the Konza prairie grassland, the location of FIFE. At the FIFE site, midday R_n and Q_a were lower when the soil was wet in 1987 [*Betts and Ball*, 1998, Table 1]. In contrast, both R_n and Q_a were higher when the soil was wet in 1988. Averaged over the two years, Q_a was only ~5 W m^{-2} higher when volumetric soil moisture was >29% than when it was <18.5%. Comparing the FIFE data to the results reported here is not straightforward. The midday averaging periods and cutoffs for the wet and dry soil composites differ. However, the Q_a response in Sevilleta shrubland and grassland is ~5 times stronger than in Konza prairie, suggesting that a significant difference exists between these environments.

[49] We hypothesize that the response of R_n and Q_a to soil moisture variations ($dQ_a/d\theta$) is greater in semiarid environments than in other regions. In semiarid areas, EF increases dramatically following rainfall events as the surface soil becomes wet, for two reasons. First, the direct soil evaporation component of ET is large because there are extensive areas of bare soil. Second, the transpiration response to individual rainfall events is substantial in many semiarid ecosystems. In the Sevilleta, EF increases from <0.1 to values as high as 0.7 following storms [*Small and Kurc*, 2001]. Similar variations are observed in the Sahel [*Taylor*, 2000]. In comparison, EF in the Konza Prairie typically varies between 0.5 and 0.8 throughout the summer, with some lower values observed during drought [*Betts and Ball*, 1998]. EF variations at the Duke Forest are similar [*Katul et al.*, 2001] (see http://www.env.duke.edu/other/AMERIFLUX/amerflux.html). The relatively large EF fluctuations in semiarid environments yield large variations in surface temperature (Figure 8), which in turn influences R_n and Q_a via the influence of surface temperature on longwave radiation emitted at the surface.

[50] **Acknowledgments.** This work was partially funded by NAG59328 from the NASA Earth Science Enterprise. This material is based on work supported in part by SAHRA (Sustainability of semi-Arid Hydrology and Riparian areas) under the STC Program of the National Science Foundation, agreement 9876800. The research at Duke Forest was supported by the Biological and Environmental Research (BER) Program, U.S. Department of Energy, through the Southeast Regional Center (SERC) of the National Institute for Global Environmental Change (NIGEC).

References

Andre, J. C., P. Bougeault, and J. P. Goutorbe, Fluxes over non-homogeneous terrain: Examples from the HAPEX-MOBILHY Programme, *Boundary Layer Meteorol.*, *50*, 77–108, 1990.

Betts, A. K., Idealized model for equilibrium boundary layer over land, *J. Hydrometeorol.*, *1*, 507–523, 2000.

Betts, A. K., and J. H. Ball, FIFE surface climate and site-average dataset 1987–1989, *J. Atmos. Sci.*, *55*, 1091–1108, 1998.

Bhark, E. W., and E. E. Small, Association between plant canopies and the spatial variability of infiltration in shrubland and grassland of the Chihuahuan desert, New Mexico, *Ecosystems*, *6*, 185–196, 2003.

Brubaker, K. L., D. Entekhabi, and P. S. Eagleson, Estimation of continental precipitation recycling, *J. Clim.*, *6*, 1077–1089, 1993.

Campbell, G. S., and J. M. Norman, *An Introduction to Environmental Biophysics*, 281 pp., Springer-Verlag, New York, 1998.

Charney, J. G., Dynamics of deserts and drought in the Sahel, *Q. J. R. Meteorol. Soc.*, *101*, 193–202, 1975.

Eltahir, E. A. B., A soil moisture-rainfall feedback mechanism: 1. Theory and observations, *Water Resour. Res.*, *34*(4), 765–776, 1998.

Eltahir, E. A. B., and R. L. Bras, Precipitation recycling, *Rev. Geophys*, *34*, 367–378, 1996.

Eltahir, E. A. B., and J. S. Pal, Relationship between surface conditions and subsequent rainfall in convective storms, *J. Geophys. Res.*, *101*, 26,237–26,245, 1996.

Entekhabi, D., and I. Rodriguez-Iturbe, Analytical framework for the characterization of the space-time variability of soil moisture, *Adv. Water Resour.*, *17*, 35–45, 1994.

Entekhabi, D., I. Rodriguez-Iturbe, and R. Bras, Variability in large-scale water balance and land surface-atmosphere interaction, *J. Clim.*, *5*, 798–813, 1992.

Ferre, P. A., J. H. Knight, D. L. Rudolph, and R. G. Kachanosi, The sample areas of conventional and alternative time domain reflectometry probes, *Water Resour. Res.*, *34*, 2971–2979, 1998.

Findell, K. L., and E. A. B. Elathir, An analysis of the soil moisture-rainfall feedback, based on direct observations from Illinois, *Water Resour. Res.*, *33*, 725–735, 1997.

Fritschen, L. J., P. Qian, E. T. Kanemasu, D. Nie, E. A. Smith, J. B. Stewart, S. B. Verma, and M. L. Wesely, Comparisons of surface flux measurement systems used in FIFE 1989, *J. Geophys. Res.*, *97*, 18,697–18,713, 1992.

Gash, J. H. C., and C. A. Nobre, Climatic effects of Amazonian deforestation: Some results from ABRACOS, *Bull. Am. Meteorol. Soc.*, *78*(5), 823–830, 1997.

Grover, H. D., and H. B. Musick, Shrubland encroachment in southern New Mexico, U.S.A.: Sn analysis of desertification processes in the American southwest, *Clim. Change*, *17*, 305–330, 1990.

Higgins, R. W., K. C. Mo, and Y. Yao, Interannual variability of the U.S. summer precipitation regime with emphasis on the southwestern monsoon, *J. Clim*, *11*, 2582–2606, 1998.

Katul, G. G., C.-T. Lai, J. D. Albertson, B. Vidakovic, K. V. R. Schäfer, C.-I. Hsieh, and R. Oren, Quantifying the complexity in mapping energy inputs and hydrologic state variables into land-surface fluxes, *Geophys. Res. Lett.*, *28*, 3305–3307, 2001.

Kimball, B. A., R. D. Jackson, F. S. Nakayama, S. B. Idso, and R. J. Reginato, Soil-heat flux determination: Temperature gradient method with computed thermal conductivities, *Soil Sci. Soc. Am. J.*, *40*, 25–28, 1976.

Kustas, W. P., J. H. Prueger, J. L. Hatfield, K. Ramalingam, and L. E. Hipps, Variability in soil heat flux from a mesquite dune site, *Agric. For. Meteorol.*, *103*, 249–264, 2000.

Lean, J., and D. A. Warrilow, Simulation of the regional climatic impact of Amazon deforestation, *Nature*, *342*, 411–413, 1989.

Rabin, R. M., S. Stadler, P. J. Wetzel, D. J. Stensrud, and M. Gregory, Observed effects of landscape variability on convective clouds, *Bull. Am. Meteorol. Soc.*, *71*, 272–280, 1990.

Sellers, P. J., F. G. Hall, G. Asrar, D. E. Strebel, and R. E. Murphy, An overview of the First International Satellite Land Surface Climatology Project (ISLSCP) Field Experiment (FIFE), *J. Geophys. Res.*, *97*, 18,345–18,371, 1992.

Shukla, J., and Y. Mintz, Influence of land-surface evapotranspiration of the Earth's climate, *Science*, *215*, 1498–1501, 1982.

Shukla, J., C. Nobre, and P. Sellers, Amazon deforestation and climate change, *Science*, *247*, 1322–1325, 1990.

Shuttleworth, W. J., The Modellion Concept, *Rev. Geophys.*, *29*, 585–606, 1991.

Small, E. E., The influence of soil moisture anomalies on variability of the North American monsoon system, *Geophys. Res. Lett.*, *28*, 139–142, 2001.

Small, E. E., and S. Kurc, The influence of soil moisture on the surface energy balance in semiarid environments, *Tech. Completion Rep. 318*, N. M. Water Resour. Res. Inst., Las Cruces, 2001.

Taylor, C. M., The influence of antecedent rainfall on Sahelian surface evaporation, *Hydrol. Processes*, *14*, 1245–1259, 2000.

Topp, G. C., J. L. Davis, and A. P. Annan, Electromagnetic determination of soil water content: Measurements in coaxial transmission lines, *Water Resour. Res.*, *16*, 574–582, 1980.

Trenberth, K. E., Atmospheric moisture recycling: Role of advection and local evaporation, *J. Clim.*, *12*, 1368–1381, 1998.

Tucotte, D. L., and G. Shubert, *Geodynamics: Applications of Continuum Physics to Geological Problems*, 450 pp., John Wiley, Hoboken, N. J., 1982.

Zheng, X., and E. A. B. Eltahir, A soil moisture-rainfall feedback mechanism: 2. Numerical experiments, *Water Resour. Res.*, *34*(4), 777–785, 1998.

S. A. Kurc and E. E. Small, Department of Geological Sciences, University of Colorado, Campus Box 399, 2200 Colorado Avenue, Boulder, CO 80309-0399, USA. (eric.small@colorado.edu)